Deoxyribonucleic Acid and Bovine Serum Albumin Interaction with the Asymmetric Schiff Base Ligand and Its Molybdenum (VI) Complex: Multi Spectroscopic and Molecular Docking Studies

Iman Khosravi, Mehdi Sahihi, Maryam Dashtbani, Hadi Amiri Rudbari, Ghazal Borhan

Deoxyribonucleic acid and bovine serum albumin interaction with the asymmetric Schiff base ligand and its molybdenum (VI) complex: multi spectroscopic and molecular docking studies

Iman Khosravi[a,*], Mehdi Sahihi[b,*], Maryam Dashtbani[b], Hadi Amiri Rudbari[b], Ghazal Borhan[c]

[a]Department of Chemistry, Qeshm Branch, Islamic Azad University, Qeshm, Iran

[b]Department of Chemistry, University of Isfahan, Isfahan 81746-73441, Iran

[c]Clinical Laboratory, Health Center No. 2, Isfahan University of Medical Science, Isfahan, Iran

***Corresponding authors** 1) Dr. Mehdi Sahihi, Tel.: +98-313-7934918, Fax: +98-313-36689732, E-mail: m.sahihi@chem.ui.ac.ir

2) Dr. Iman Khosravi, Tel.: +98-915-501-6303, E-mail:iman.khos2012@gmail.com

E-mails of co-authors:

h.a.rudbari@sci.ui.ac.ir

maryam.dashtbani70@yahoo.com

gh_b2003@yahoo.it

Abstract

The interaction of an asymmetric Schiff base ligand derived from allylamine and 2,3-dihydroxybenzaldehyde and its molybdenum (VI) complex with deoxyribonucleic acid (DNA) and bovine serum albumin (BSA) were studied using spectroscopic and molecular docking methods. The spectroscopic results revealed that the DNA and BSA affinity for binding the Mo(VI) complex is greater than its ligand. Furthermore, the molecular docking calculations

showed that H-bond, hydrophobic, π-π and π-cation interactions had the dominant role in the stability of the compound-BSA complexes. The DNA interaction results suggested that the compounds interacted with DNA by the groove binding mechanism.

Keyword

DNA interaction, BSA binding, Fluorescence quenching, Molecular docking, Schiff base.

1. Introduction

Schiff bases are a class of compounds that have attracted a large number of researchers due to their easy formation, high stability, their pharmacological properties and, notably, anti-cancer activity [1-4]. Also, in recent years, remarkable attention has been paid to the biological applications of the metal complexes of Schiff bases due to their stability, biocompatibility and biological activity [5,6]. Biochemists believe that the cause of the biological activity of these compounds is the imine group existence in the chemical structure of Schiff bases [7-9]. Furthermore, results of recent investigations indicated that after complexation of Schiff base ligands with transition metal ions, their biological activity was enhanced [10-12]. Therefore, investigation of their interaction with biomacromolecules, such as DNA and proteins, is the first step for the intellectual design and fabrication of new and more efficient pharmaceutical molecules. Proteins are vital and impartible members of our life and a major target in medicine and pharmacy fields, similar to DNA. The interaction mechanism of a drug with plasma proteins is a key point to understanding the drugs pharmacodynamics and pharmacokinetics [13]. Generally, proteins are known as the major targets for most of the drugs used in organisms [14]. Their interaction with a drug affects the drug absorption, distribution and elimination in the circulatory system [15], and can prevent its rapid elimination from the blood stream [16]. Bovine serum albumin (BSA) is the most abundant plasma protein; it also is known as the dominant transporter plasma protein for endogenous and exogenous ligands (fatty acids, hormones and drugs) [17]. The BSA-binding of a drug can increase its solubility in plasma, decrease its toxicity, protect it from oxidation, prolong its *in-vivo* half-life as well as increase the pharmaceutical effect of the drug [18].

As a part of our ongoing investigation into designing new Schiff base ligands and complexes [19-23], and studying their interaction with biomacromolecules, herein the DNA- and BSA-binding of the asymmetric Schiff base ligand derived from allylamine and 2, 3-dihydroxybenzaldehyde (**L**) and its molybdenum(VI) complex (**MoL_2**) (Fig. 1), which had been synthesized in our research group earlier [21], was evaluated using both experimental (fluorescence quenching and UV--Vis spectroscopy) and computational methods (molecular docking).

2. Experimental

2.1. Chemicals and instrumentation

All the chemicals for synthesis of the compounds were purchased from the Merck Co. (Germany) and used without further purification. BSA and DNA were purchased from the Sigma-Aldrich Corp. (France). All used salts for buffer preparation were analytical grade and were dissolved in double distilled water. All of the solutions were used freshly after preparation. The UV-Vis spectra were recorded on a V-670 spectrophotometer (Jasco Inc., Japan). Fluorescence quenching experiments were carried out at room temperature using RF-5000 spectrofluorometer (Shimadzu Corp., Japan).

2.2. BSA binding experiments

2.2.1. Preparation of L and ML_2 compounds and protein stock solutions

A stock solution of BSA was prepared by dissolving the desired amount of BSA in 50 mM phosphate buffer (pH = 7). The BSA stock solution was stored at 4°C in the dark and was used within 2 h. The BSA concentration was determined by UV-Vis

spectrophotometry using the molar absorption coefficient 44300 $M^{-1}cm^{-1}$ at 280 nm [24]. The solutions of the L and ML_2 compounds were first prepared in DMF and then were diluted suitably, with phosphate buffer to the required concentrations for all the experiments. The volume of DMF never exceeded 0.5% (v/v), so the effect of DMF was negligible. All the solutions were used freshly after preparation.

2.2.2. Fluorescence spectroscopy measurements

The interactions of BSA with the **L** and **MoL_2** were investigated using fluorescence quenching experiments. In this experiment 2 mL of BSA solution (5 μM) was placed into the cell and various amounts of the **L** and **MoL_2** compounds (0-50 μM) were added to it. The fluorescence intensity was measured with an excitation wavelength at 295 nm and emission wavelength range of 300-450 nm. In each measurement the mixture was allowed to incubate for 2 min after addition of the compounds to the cell. Moreover, the measured fluorescence intensities were corrected for the dilution and the inner filter effects.

2.2.3. UV-Vis absorption spectroscopy measurements

Electronic absorption spectroscopy is one of the methods used for studying the binding modes of drugs to biomacromolecules**.** Absorption titration experiment was carried out to further investigate the BSA-binding of the compounds at room temperature. The UV-Vis absorption spectra of the solution of BSA (10 μM) in the absence and presence of 1-100 μM of **L** and **MoL_2** were recorded at room temperature and the changes in the BSA absorption were recorded after each addition of the ligand or complex. Absorption curves of the compounds--protein mixtures were corrected by subtracting the spectra of the **L** and

MoL_2 solutions. All intensities were corrected for the dilution effect in the UV absorption experiments.

2.3. DNA binding studies

2.3.1. Preparation of compounds and Fish Sperm DNA (FS-DNA) stock solutions

The stock solution of FS-DNA was prepared in 50 mM Tris buffer at pH 7.5 using double-distilled deionized water and stored at 4 ˚C. The FS-DNA concentration per nucleotide was determined using the absorption intensity at 260 nm after adequate dilution with the buffer and using the reported molar absorptivity of 6600 $M^{-1}.cm^{-1}$. The purity of the FS-DNA solution was confirmed by the ratio of UV absorbance at 260 and 280 nm with a value of A_{260}/A_{280} = 1.9 indicating that the FS-DNA was free from protein impurity [25]. The solutions of the compounds were first prepared in DMF as co-solvent, and then diluted with the corresponding Tris buffer to the required concentration for all experiments. The volume of the co-solvent never exceeded 0.5% (v/v), so the effect of the DMF was negligible.

2.3.2. Fluorescence spectroscopic measurements

Fluorescence quenching experiments were carried out using a quartz cuvette with 1 cm optical path length; the excitation and emission slits were set at 5 and 10 nm, respectively. For this purpose the FS-DNA solution was stirred with ethidium bromide (EtBr), with molar ratio of DNA:EtBr 10:1, for 1 h at 4°C. Then various amounts of the Mo complex (0--250 μM) were added to this mixture. The fluorescence spectra were measured in the range of 500--700 nm with exciting wavelength at 520 nm. In each measurement, after addition of FS-DNA, the mixture was allowed to stand for 2 min prior to the measurements. Moreover, the measured fluorescence intensities were corrected for the dilution and inner-filter effects.

2.3.3. UV-Vis spectroscopy measurements

Absorption titration experiments were carried out to further investigate the DNA-binding of the compounds at room temperature. Absorption spectral titration experiments were performed by addition of various amounts of FS-DNA-Tris buffer solution (0-5 × 10^{-5} M) to the L and ML_2 compounds-Tris buffer solutions (1 × 10^{-5} M). All compounds--DNA solutions were allowed to incubate for 2 min before recording the related spectra. Absorption curves of the compounds--DNA mixtures were corrected by subtracting the spectrum of DNA and all intensities were corrected for the dilution effect.

2.4. Molecular docking procedure

Study of the interaction between drug molecules and biomacromolecules is one of the interesting topics in biochemistry [26]. Molecular docking helps investigations of these interactions. Owing to this, we examined the docking of **L** and $\mathbf{MoL_2}$ with BSA and DNA, as important biomacromolecules. The 3D structures of the **L** and $\mathbf{MoL_2}$ were obtained using the. cif (Crystallographic Information File) files of their X-ray crystal structures [21]. The .cif files were converted to the .pdb (Protein Data Bank) format by using the Mercury software (http://www.ccdc.cam.ac.uk/). The crystal structure of BSA (PDB ID: 4F5S) and DNA (PDB ID: 423D) with sequence $d(ACCGACGTCGGT)_2$ were taken from the Brookhaven Protein Data Bank (http://www.rcsb.org/pdb). The resolution of these files were 2.47 and 1.6 Å for BSA and DNA, respectively. Water molecules in the structures of the .pdb files were deleted and missing hydrogen atoms were added. Flexible-ligand docking was carried out by the AutoDock 4.2.5.1 molecular-docking

program (http://autodock.scripps.edu/) using the implemented empirical free energy function and the Lamarckian Genetic Algorithm [27]. The Gasteiger (Gasteiger-Marsili) charges were added to prepare the macromolecule input file for docking and the Auto Grid was used to calculate Grids. For the docking of **L** and **MoL_2** to BSA and DNA, a blind docking with 126 lattice points along each of the X, Y, and Z axes was performed to find the binding sites of the compounds on BSA and DNA with a grid point spacing of 0.375 Å, to allow the compounds to rotate freely. In the next step, the center of the grid box was located at the binding site and a second docking was performed using a cubic box with 60 × 60 × 60 dimensions. 250 docking runs with 25,000,000 energy evaluations for each run were performed.

3. Results and Discussion

3.1. Interactions with Bovine Serum Albumin (BSA)

Serum albumin (SA) is one of the most important targets in binding of various molecules such as drugs (warfarin, diazepam, Ibuprofen) [28], metal ions [29], fatty acids [30], etc. SA is recognized as a transporter protein of blood plasma. Hence, in recent years much attention has been focused on drug-SA interactions. Understanding of these interaction mechanisms help us to know the pharmacodynamics and pharmacokinetics effects of drugs. Several experimental and computational methods have been used to study these binding processes. In the current study the BSA-binding of the prepared compounds was investigated using both experimental and theoretical methods.

3.1.1. Fluorescence spectroscopy.

Fluorescence spectroscopy is a sensitive and effective method to study the binding of drugs to biomacromolecules. A fluorescence quenching experiment can characterize the availability of quenchers to protein fluorophore, which helps us to obtain the binding mode, binding constants, number of binding sites and intermolecular distances [31]. The fluorescence intensity of the protein was quenched through the addition of the synthesized compounds. This implies that the compounds strongly interacted with BSA, leading to changes of the microenvironment around the Trp residues in BSA [32,33]. Fig. 2 indicates the fluorescence quenching of 5×10^{-6} M BSA in the presence of 0.5-50 μM of the compounds.

In order to determine the binding ability between the compounds and BSA, the Stern--Volmer quenching plot was obtained by monitoring the fluorescence quenching of BSA with increasing concentration of the compounds, according to the Stern--Volmer equation [34]:

$$\frac{F_0}{F} = 1 + K_{sv}[Q] = 1 + k_q \tau [Q] \quad (1)$$

where F_0 and F are the fluorescence intensity of BSA in the absence and presence of the compounds. K_{sv} is the Stern-Volmer quenching constant, k_q is the quenching rate constant of BSA and τ is the average lifetime of BSA without quencher which is typically equal to 10^{-8} s for biomacromolecules [35]. K_{sv} is determined from the plot of F_0 / F vs. [Q] (insets in Fig. 2). In the present study the values of K_{sv} were obtained and are listed in Table 1.

Fluorescence quenching is proposed to occur according to one of two mechanisms: static quenching and dynamic quenching. In the static mechanism, while the fluorophore and the quencher collide together in the ground state while the fluorophore and quencher collide together in the excited state in the dynamic mechanism [35]. Linearity of the Stern-Volmer plot indicates that the quenching fluorescence has only one mechanism, dynamic or static [36]. The value of k_q was obtained and is also listed in Table 1. In this study, the values of k_q were greater than the limiting diffusion rate constant for the diffusional quenching for biopolymers (2×10^{10} $M^{-1}.S^{-1}$); this observation supports that the quenching fluorescence of BSA occurred by the static mechanism.

The affinity of the biomacromolecules for binding the drugs can be stated by the equilibrium constant (binding constant) for "drug + biomacromolecule↔ drug-biomacromolecule complex" equlilibrium. The binding constants (K_b) were determined using the following equation [36]:

$$Ln\left(\frac{F_0 - F}{F}\right) = Ln(K_b) + nLn[Q] \quad (2)$$

where F_0 and F are the fluorescence intensity of BSA in the absence and presence of the compounds, respectively. [Q] is the concentration of quencher; i.e., the synthesized compounds here. "K_b" is obtained from the plot of $\mathrm{Ln}((F_0 - F)/F)$ versus Ln[Q] as the y-intercept (figures not shown). The K_b values revealed that the **MoL$_2$**-BSA complex was more stable than the **L**-BSA; in other words, the **MoL$_2$**-BSA complex was more available for drug-cell interaction. Moreover, this result was in good agreement with the UV-Vis spectroscopy and molecular docking results. Furthermore, "*n*", which is the number of

binding sites per protein molecules, is the slope of the plot. The value of *n* was nearly 1, indicating that the synthesized compound binds to BSA with a molar ratio of 1:1. The calculated results are shown in Table 1.

In general, the binding constant of a drug with a carrier protein, such as BSA, should be high enough to bind sufficiently to permit transfer through the body. Moreover, in order to release a drug following arrival at its target, it should not be too high. With respect to the above, the BSA-binding constants of both compounds were in a good range (1-6 × 10^4 M^{-1}) [37]. In addition, our compounds were in an uncharged form which is an advantage for a drug; research has shown that a unionized drug is soluble in lipid and capable of crossing through the membrane's lipid bilayer while the ionized analogue species fail to cross [38]. The obtained results show that **L** and **MoL_2** bind to BSA differently, confirming the effect of the metal ion on the affinity of the two compounds to BSA.

3.1.2. UV-Vis absorption.

UV-Vis absorption spectroscopy is a useful technique that has been frequently used to examine binding processes. The absorption titration was carried out by adding various amounts of **L** or **MoL_2** compound to the BSA ([Compound]/[BSA] = 0-4.5); their absorption spectra are shown in Fig. 3. Through addition of various amounts of the compounds, a hypochromic effect in the spectrum of BSA was observed. In order to assess the binding ability of the two compounds with BSA, the intrinsic binding constant (K_b) was estimated by monitoring the changes of absorbance with increasing concentration of compounds and using the following equation [40]:

$$\frac{1}{(A - A_0)} = \frac{1}{(A_{max} - A)} + \frac{1}{K_b (A_{max} - A)} \times \frac{1}{[M]} \quad (3)$$

where, A_0 and A are the absorbance of BSA in the absence and presence of the compound, respectively. A_{max} is the obtained absorbance at saturation and [M] is the concentration of the compound. The plot of $1/(A-A_0)$ versus 1/[M] gives K_b as the ratio of the y-intercept to the slope (Table 1). The binding constants for **L** and **MoL_2** are equal to 1.4×10^3 and 2.9×10^3 M^{-1}, respectively.

3.1.3. Energy transfer from BSA to compounds.

Knowledge of the energy transfer between the compounds and BSA can provide valuable information about the BSA-complex binding. The change in the fluorescence quenching of BSA upon its binding to **L** and **MoL_2** can be indicative of energy transfer between BSA and the compounds. This energy transfer can be explained by the fluorescence resonance energy transfer (FRET) theory. FRET, also known as Förster's resonance energy transfer; it is the result of an interaction between the excited molecule and its adjacent molecule. Upon this interaction, the absorbed energy by the donor molecule is transferred to an acceptor [19]. According to this theory, three conditions are required for energy transfer: (1) the donor should have fluorescence, (2) the fluorescence emission spectrum of the donor and the UV-Vis spectrum of the acceptor should have sufficient overlap (3) a small distance between donor and acceptor (< 8 nm) [19]. The distance (*r*) and efficiency of energy transfer (*E*) between the tryptophan residue of the protein (BSA) and drug (**L** and **MoL_2**) was calculated using this theory through the following equation:

$$E = 1 - \frac{F}{F_0} = \frac{R_0^6}{R_0^6 + r^6} \quad (4)$$

where F_0 and F are fluorescence intensities of BSA in the absence and presence of the complex, respectively, R_0 is the critical distance when the transfer efficiency is 50% and r is the distance between donor and acceptor. R_0 can be calculated by Eq. (5) [41].

$$R_0^6 = 8.79 \times 10^{-25} K^2 N^{-4} J \varphi \quad (5)$$

In the above equation, the term K^2 is the orientation factor of the dipoles; N is the refractive index of medium, J is the overlap integral of the fluorescence spectrum of the donor with the absorption spectrum of the acceptor and φ is the fluorescence quantum yield of the donor. The value of J can be calculated by the following expression:

$$J = \left[\sum F(\lambda)\varepsilon(\lambda)\lambda^4 \Delta\lambda\right] / \left[\sum F(\lambda)\Delta\lambda\right] \quad (6)$$

where *F(λ)* is the fluorescence intensity of the donor in the absence of the acceptor at wavelength λ and ε is the molar absorption coefficient of the acceptor at λ. In the present case $K^2 = 2/3$, N = 1.336 and $\varphi = 0.15$ for BSA. Fig. 4 revealed that there is sufficient overlap between emission spectrum of BSA and absorption spectrum of the compounds. Therefore, according to Eqs. (4-6) the parameters for the synthesized compounds were calculated and the related results are listed in Table 2 and Figure 4. The values of *r* for both compounds were less than 8 nm and $(0.5\ R_0) < r < (1.5\ R_0)$, suggesting energy transfer from BSA to the compounds occurred with high probability.

3.1.4. Docking study.

One of the known theoretical techniques in biochemistry that can give us information about the atomic details of the interaction of various molecules with biomacromolecules

is molecular docking. Therefore, the synthesized compounds were docked to the conformation of BSA in its crystal. The docking results are shown in Fig. 5; it shows that **MoL_2** and **L** were bound to the IIIB subdomain of BSA. The interactions of the compounds within the binding sites of BSA are also shown in this figure. The binding site is considerably hydrophobic, so the **L** and **MoL_2** were in hydrophobic interaction with hydrophobic residues in their binding site. Also, Fig. 5a shows that there were two hydrogen bond interactions of **MoL_2**, with Tyr 419 and one with Lys 533 residues. Furthermore, two π-cation interactions with Lys 499 stabilized the **MoL_2**--BSA complex. Figure 5b shows that **L** is in hydrogen bond interaction with Ala 527 residue and π-π interactions with Phe 550 residue. The obtained binding energies for the compound-BSA systems are listed in Table 1. The larger negative value of binding energy for **MoL_2** means a higher affinity for BSA binding, which is in good agreement with the UV-Vis and fluorescence experimental data.

3.2. Interaction with DNA

3.2.1. Fluorescence spectroscopy

The fluorescence measurements were performed to further investigate the interaction mode between the synthesized compounds and FS-DNA (Fig. 6). Hydrogen transfer from one of the amino groups of ethidium bromide (EtBr) into the solution caused nonradiative decay and a weak fluorescence emission. However, a significant increase of fluorescence intensity of EtBr was observed in the presence of FS-DNA due to intercalation of the EtBr molecules into the double helix of the DNA [42-45]. Figure 6 represents the fluorescence enhancement of the DNA-EtBr by addition of the compounds. In order to

determine the binding ability between the compounds and FS-DNA, the enhancement plot was obtained by monitoring the fluorescence enhancement of EtBr-DNA with increasing concentration of the compounds according to the equation (6) [46].

$$\frac{F}{F_0} = 1 + K_E [E] \quad (6)$$

where F_0 and F are the fluorescence intensity of the EtBr-DNA complex in the absence and presence of the compounds. K_E is the enhancement constant and [E] is the concentration of the enhancer that causes the enhancement of fluorescence intensity (**L** and **MoL$_2$**). The values of K_E for the synthesized compounds were determined from the plot of F/F_0 vs. [Q] (Fig. 6) and are presented in Table 3. In this study, the binding constants (K_b) for the interaction of **L** and **MoL$_2$** with FS-DNA were determined using equation (7) and are presented in Table 3 [46].

$$Ln\left(\frac{F - F_0}{F}\right) = Ln(K_b) + nLn[E] \quad (7)$$

where F_0 and F are the fluorescence intensity of EtBr-DNA in the absence and presence of the compounds, respectively. [E] is the concentration of enhancer; i.e., the synthesized compounds here. "K_b" is obtained from the plot of $Ln((F_0 - F)/F)$ versus Ln[E] as the y-intercept (Figures are not shown).The K_b values reveal that the **MoL$_2$** formed a more stable complex with FS-DNA than **L**.

3.2.2. UV-Vis absorption

The absorption spectra of **L** and **MoL_2** in the absence and presence of various concentrations of FS-DNA are given in Fig. 7. The intensity of these spectra decreased with the addition of FS-DNA. To quantitatively evaluate the affinity of the compounds with FS-DNA, the intrinsic binding constant K_b was determined by monitoring the changes in absorbance using equation (8).

$$\frac{1}{(\varepsilon_a - \varepsilon_f)} = \frac{1}{(\varepsilon_b - \varepsilon_f)} + \frac{1}{K_b(\varepsilon_b - \varepsilon_f)} \times \frac{1}{[DNA]} \quad (8)$$

where ε_a, ε_f and ε_b are the apparent extinction coefficient, the extinction coefficient for free compounds and the extinction coefficient for the compound in the fully bound form, respectively. ε_f was determined based on the calibration curve and ε_a is the ratio of A_{obs} to [compound]. The plot of $1/(\varepsilon_a-\varepsilon_f)$ versus 1/[DNA] gives K_b as the ratio of the y-intercept to slope (insets in Fig. 7). The binding constants for **L** and **MoL_2** were about 1.7×10^3 and 1.9×10^3 M^{-1}, respectively.

3.2.3. Docking study

Molecular docking studies were carried out to obtain a deeper insight into the DNA binding of **L** and **MoL_2**. The docking results revealed that **L** and **MoL_2** were bound to the minor groove of DNA. Figures 8a and 8b present the binding modes and the nucleotides around **MoL_2** and **L**, respectively. The molecular docking results show hydrogen bond interactions for **L** and **MoL_2** in the minor groove of DNA. The standard binding free energies ($\Delta G°$), describing the affinity of the **L** and **MoL_2** for binding to DNA with the best scores, were -5.50 and -8.77 kcal.mol^{-1}, respectively. The docking results were in good agreement with the spectroscopic results. Both the experimental results and

computational docking data, collectively, suggested that the **MoL_2** complex had more DNA binding affinity than the **L** Schiff base ligand.

4. Conclusions

The DNA- and BSA- binding of an asymmetric Schiff base ligand derived from allylamine and 2, 3-dihydroxybenzaldehyde and its molybdenum (VI) complex are described. These compounds had been previously synthesized in our research group [21] and were resynthesized using the same procedure. The DNA binding results indicate that the both compounds interact with DNA, presumably by the groove binding mechanism; the Mo(VI) complex exhibited stronger DNA binding affinity compared to the Schiff base ligand. The BSA-binding of the synthesized compounds were also evaluated, using experimental (fluorescence quenching and UV-Vis spectroscopy) as well as computational methods (molecular docking). The obtained results indicated that the Mo(VI) complex also bound to BSA stronger than the Schiff base ligand. The calculated binding constants between these compounds and BSA were about 10^4 M^{-1}. The results of the fluorescence experiment as well as the changes in the absorption spectra of the compounds upon addition of the BSA show that the BSA-compound complexes formed in the ground state. In addition, molecular docking studies revealed that hydrogen bond interactions, hydrophobic interactions, π - π stacking and π-cation interactions have the dominant roles in the interaction of these compounds with BSA. Generally, the results of the present study exhibited the effect of the metal ion on the DNA- and BSA-binding of the drugs and their values of binding constants.

Acknowledgement

The authors are grateful to the Research Council of the Islamic Azad University (Qeshm branch) for financial support of this work.

References:

[1] Ferlay, J. Soerjomataram, I. Ervik, M. Dikshit, R. Eser, S. Mathers, C. Rebelo, M. Parkin, D.M. Forman, D. Bray, F. *Cancer Incidence and Mortality Worldwide*, International Agency for Research on Cancer, Lyon, **2013**

[2] Chow, M.J. Licona, C. Wong, D.Y.Q. Pastorin, G. Gaiddon, C. Ang, W.H. Discovery and Investigation of Anticancer Ruthenium--Arene Schiff-Base Complexes via Water-Promoted Combinatorial Three-Component Assembly. *J. Med. Chem.* **2014**, 57, 6043--6059.

[3] Chen, W. Ou, W. Wang, L. Hao, Y. Cheng, J. Li, J. Liu, Y.N. Synthesis and biological evaluation of hydroxyl-substituted Schiff-bases containing ferrocenyl moieties. *Dalton Trans*. **2013**, 42, 15678- 15686.

[4] Ghosh, M. Layek, M. Fleck, M. Saha, R. Bandyopadhyay, D. Synthesis, crystal structure and antibacterial activities of mixed ligand copper(II) and cobalt(II) complexes of a NNS Schiff base *Polyhedron*, **2015**, 85,312-319.

[5] Pravin, N. Raman, N. Investigation of in vitro anticancer and DNA strap interactions in live cells using carboplatin type Cu(II) and Zn(II) metalloinsertors. *Eur. J. Med. Chem*. **2014**, 85, 675-687.

[6] Arjmand, F. Sayeed, F. Muddassi, M. Synthesis of new chiral heterocyclic Schiff base modulated Cu(II)/Zn(II) complexes: Their comparative binding studies with CT-DNA,

mononucleotides and cleavage activity. *J. Photochem. Photobiol. B: Biology*. **2011**, 103, 166-179.

[7] Raman, N. Selvan, A. Sudharsan, S. Metallation of ethylenediamine based Schiff base with biologically active Cu(II), Ni(II) and Zn(II) ions: Synthesis, spectroscopic characterization, electrochemical behaviour, DNA binding, photonuclease activity and in vitro antimicrobial efficacy. *Spectrochim. Acta Part A: Mol. Biomol. Spect.* **2011**, 79, 873-883.

[8] Antony, R. Manickam, S.T.D. Saravanan, K. Karuppasamy, K. Balakumar, S. Synthesis, spectroscopic and catalytic studies of Cu(II), Co(II) and Ni(II) complexes immobilized on Schiff base modified chitosan. *J. Mol. Struct*. **2013**, 1050, 53-60.

[9] Guo, Z.Y. Xing, R. Liu, S. Zhong, Z. Ji, X. Wang, L. Li, P.C. Antifungal properties of Schiff bases of chitosan, N-substituted chitosan and quaternized chitosan. *Carbohyd. Res*. **2007**, 342, 1329-1332.

[10] Anacona, J.R. Rodriguez, J.L. Camus, Synthesis, characterization and antibacterial activity of a Schiff base derived from cephalexin and sulphathiazole and its transition metal complexes. *Spectrochim. Acta Part A: Mol. Biomol. Spect.* **2014**, 129, 96-102.

[11] Sundararajana, M.L. Jeyakumar, T. Anandakumaran, J. Karpanai, B. Synthesis of metal complexes involving Schiff base ligand with methylenedioxy moiety: Spectral, thermal, XRD and antimicrobial studies. *Spectrochim. Acta Part A: Mol. Biomol. Spect.* **2014**, 131, 82-93.

[12] Tarushi, A. Polatoglou, E. Kljun, J. Turel, I. Dimitris, G.P. Kessissoglou, P. Interaction of Zn(II) with quinolone drugs: Structure and biological evaluation. *Dalton Trans*. **2011**, 40, 9461-9473.

[13] Cui, F. Qin, L. Zhang, G. Lio, Q. Yao, X. Lei, B. Interaction of anthracycline disaccharide with human serum albumin: Investigation by fluorescence spectroscopic technique and modeling studies. *J. Pharm. Biomed. Analy.* **2008**, 48, 1029-1036.

[14] Vuignier, K. Schappler, J. Veuthey J.L. Carrupt, P.A. Martel S. Drug--protein binding: a critical review of analytical tools. *Anal. Bioanal. Chem.* **2010**, 398, 53-66.

[15] McCallum, M.M. Pawlak, A.J. Shadrick, W.R. Simeonov, A. Jadhav, A. Yasgar, A. Maloney, D.J. Arnold, L.A. A fluorescence-based high throughput assay for the determination of small molecule−human serum albumin protein binding. *Anal. Bioanal. Chem.* **2014**, 406, 1867-1875.

[16] Li, F. Feterl, M. Warner, J.M. Day, A.I. Keene, F.R. Collins, J.G. Protein binding by dinuclear polypyridyl ruthenium(II) complexes and the effect of cucurbit [10] uril encapsulation. *Dalton Trans.* **2013**, 42, 8868-8877.

[17] Domonkos, C. Zsila, F. Fitos, I. Visy, J. Kassai, R. Bálint, B. Kotschy, A. Synthesis and serum protein binding of novel ring-substituted harmine derivatives. *RSC Adv.* **2015**, 5, 53809-53818.

[18] Gou, Y. Zhang, Y. Qi, J. Zhou, Z. Yang, F. Liang, H. Enhancing the copper(II) complexes cytotoxicity to cancer cells through bound to human serum albumin. *J. Inorg. Biochem.* **2015**, 144, 47-55.

[19] Khosravi, I. Hosseini, F. Khorshidifard, M. Sahihi, M. Amiri Rudbari, H. Synthesis, characterization, crystal structure and HSA binding of two new N,O,O-donor Schiff-base ligands derived from dihydroxybenzaldehyde and tert-butylamine. *J. Mol. Struc.* **2016**, 1119, 373-384.

[20] Khorshidifard, M. Amiri Rudbari, H. Askari, B. Sahihi, M. Riahi Farsani, M. Jalilian, F. Bruno, G. Cobalt(II), copper(II), zinc(II) and palladium(II) Schiff base complexes: Synthesis, characterization and catalytic performance in selective oxidation of sulfides using hydrogen peroxide under solvent-free conditions. *Polyhedron*. **2015**, 95, 1-13.

[21] Amiri Rudbari, H. Khorshidifard, M. Askari, B. Habibi, N. Bruno, G. New asymmetric Schiff base ligand derived from allylamine and 2,3-dihydroxybenzaldehyde and its molybdenum(VI) complex: Synthesis, characterization, crystal structures, computational studies and antibacterial activity together with synergistic effect against Pseudomonas aeroginosa PTTC 1570. *Polyhedron*. **2015**, 100, 180-191.

[22] Kazemi, Z. Amiri Rudbari, H. Sahihi, M. Mirkhani, V. Moghadam, M. Tangestaninejad, S. Mohammadpoor-Baltork, I. Gharaghani. S. Synthesis, characterization and biological application of four novel metal-Schiff base complexes derived from allylamine and their interactions with human serum albumin: Experimental, molecular docking and ONIOM computational study. *J. Photochem. Photobio. B: Biology*. **2016**, 162, 448-462.

[23] Kazemi, Z. Amiri Rudbari, H. Sahihi, M. Mirkhani, V. Moghadam, M. Tangestaninejad, S. Mohammadpoor-Baltork, I. Azimi, G. Gharaghani, S. Abbasi Kajani. A. *J. Photochem. Photobio. B: Biology*. **2016**, 163, 246-260.

[24] Anjomshoa, M. Torkzadeh-Mahani, Janczak, M. J. Rizzoli, C. Sahihi, M. Ataei, F. Dehkhodaei, Synthesis, crystal structure and Hirshfeld surface analysis of copper(II) complexes: DNA- and BSA-binding, molecular modeling, cell imaging and cytotoxicity. *Polyhedron*, **2016**, 119, 23-38.

[25] Zheng, K. Liu, F. Xu, X.M. Li, Y.T. Wu, Z.Y. Yan, C.W. Synthesis, structure and molecular docking studies of dicopper(II) complexes bridged by N-phenolato-N′-[2-(dimethylamino)ethyl]oxamide: the influence of terminal ligands on cytotoxicity and reactivity towards DNA and protein BSA. *New J. Chem.* **2014**, 38, 2964-2978.

[26] Tian, M.Y. Zhang, X.F. Xie, L. Xiang, J.F. Tang, Y.L. Zhao, C.Q. The effect of Cu2+ on the interaction between an antitumor drug--mitoxantrone and human serum albumin. *J. Mol. Struct.* **2008**, 892, 20-24.

[27] Morris, G.M. Goodsell, D.S. Halliday, R.S. Huey, R. Hart, W.E. Belew, R.K. Olson, A.J. Automated Docking Using a Lamarckian Genetic Algorithm and an Empirical Binding Free Energy Function. *J. Comp. Chem.* **1998**, 19, 1639-1662.

[28] Ghuman, J. Zunszain, P.A. Petitpas, I. Bhattacharya, A.A. Otagiri, M. Curry, S. Structural Basis of the Drug-binding Specificity of Human Serum Albumin. *J. Mol. Biol.* **2005**, 353, 38-52.

[29] Bal, W. Sokolowska, M. Kurowska, E. Faller, P. Binding of transition metal ions to albumin: Sites, affinities and rates. *Biochim. Biophys. Acta (BBA) - General Subjects*. **2013**, 1830, 5444-5455.

[30] Bhattacharya, A.A. Grune, T. Curry, S. Bhattacharya, A.A. Grune, T. Curry, S. J. Mol. Biol. 2000, 303, 721. *J. Mol. Biol.* **2000**, 303, 721-732.

[31] Fu, X.B. Liu, D.D. Lin, Y. Hu, W. Mao, Z.W. Le, X.Y. Water-soluble DNA minor groove binders as potential chemotherapeutic agents: synthesis, characterization, DNA binding and cleavage, antioxidation, cytotoxicity and HSA interactions. *Dalton Trans*. **2014**, 43, 8721-8737.

[32] Mrkalić, E.M. Jelić, R.M. Klisurić, O.R. Matović, Z.D. Synthesis of novel palladium(II) complexes with oxalic acid diamide derivatives and their interaction with nucleosides and proteins. Structural, solution, and computational study. *Dalton Trans*. **2014**, 43, 15126-15137.

[33] Wang, Y.Q. Zhang, H.M. Zhang, G.C. Tao, W.H. Tang, S.H. Interaction of the flavonoid hesperidin with bovine serum albumin: A fluorescence quenching study. *J. Lumin.* **2007**, 126, 211-218.

[34] Dighe, S.U. Khan, S. Soni, I. Jain, P. Shukla, S. Yadav, R. Sen, P. Meeran, S.M. Batra, S. Synthesis of β-Carboline-Based N-Heterocyclic Carbenes and Their Antiproliferative and Antimetastatic Activities against Human Breast Cancer Cells. *J. Med. Chem*. **2015**, 58, 3485-3499.

[35] Darabi, F. Hadadzadeh, H. Ebrahimi, M. Khayamian, T. Amiri, H. The piroxicam complex of cobalt(II): Synthesis in two different ionic liquids, structure, DNA- and BSA interaction and molecular modeling. *Inorg. Chim. Acta*. **2014**, 409, 379-389.

[36] Lakowicz, J.R. Plasmonics in Biology and Plasmon-Controlled Fluorescence. *Plasmonics*, **2006**, 1, 5-33.

[37] Kyropoulou, M. Raptopoulou, C.P. Psycharis, V. Psomas, G. Ni(II) complexes with non-steroidal anti-inflammatory drug diclofenac: Structure and interaction with DNA and albumins. *Polyhedron*. **2013**, 61, 126-136.

[38] Abou-Zied, O.K. Revealing the ionization ability of binding site I of human serum albumin using 2-(2′-hydroxyphenyl)benzoxazole as a pH sensitive probe. *Phys. Chem. Chem. Phys*. **2012**, 14, 2832-2839.

[39] Bhat, S.S. Kumbhar, A.A. Heptullah, H. Khan, A.A. Gobre, V.V. Gejji, S.P. Puranik, V.G. Synthesis, Electronic Structure, DNA and Protein Binding, DNA Cleavage, and Anticancer Activity of Fluorophore-Labeled Copper(II) Complexes. *Inorg. Chem*. **2010**, 50, 545-558.

[40] Das, A. Kumar, G.S. Binding studies of aristololactam-β-D-glucoside and daunomycin to human serum albumin. *RSC Adv.* **2014**, 4, 33082-33090.

[41] Huang, Y. Wang, S. Bi, Y. Jin, J. Ehsan, M.F. Fu, M. He, T. Preparation of 2D hydroxyl-rich carbon nitride nanosheets for photocatalytic reduction of CO2. *RSC Adv*. **2015**, 5, 33254-33261.

[42] Arjmand, F. Jamsheera, A. Mohapatra, D.K. Synthesis, characterization and in vitro DNA binding and cleavage studies of Cu(II)/Zn(II) dipeptide complexes. *J. Photochem. Photobiol. B: Biol.* **2013**, 121, 75-85.

[43] Fu, X.B. Weng, G.T. Liu, D.D. Le, X.Y. DNA binding and cleavage, HSA interaction and cytotoxicity of a new copper (II) complex derived from 2-(2-pyridyl) benzothiazole and glycylglycine. *J. Photochem. Photobiol. A: Chem.* **2014**, 276, 83-95.

[44] Waring, M.J. Complex formation between ethidium bromide and nucleic acids. *J. Mol. Biol.* **1965**, 13, 269-282.

[45] Fromherz, P. Rieger, B. Photoinduced electron transfer in DNA matrix from intercalated ethidium to condensed methylviologen. *J. Am. Chem. Soc.* **1986**, 108, 5361-5362.

[46] Shahabadi, N. Kashanian, S. Darabi, F. In Vitro Study of DNA Interaction with a Water-Soluble Dinitrogen Schiff Base. *DNA Cell Biol*. **2009**, 28, 589-596.

Table 1. BSA-binding constants, binding energy, number of binding site (n), and Stern--Volmer constant

Type of Complex	$K_{binding}/M^{-1}$ (Fluorescence)	$K_{binding}/M^{-1}$ (UV-Vis)	Binding Energy/kcal.mol^{-1} (Docking)	n	K_{sv}/M^{-1}	$k_q/M^{-1}S^{-1}$
L	1.01×10^4	1.4×10^3	-5.89	0.8671	6.2×10^3	6.2×10^{11}
MoL_2	3.4×10^4	2.9×10^3	-7.05	1.02	4.1×10^4	4.1×10^{12}

(K_{SV}) of the compounds.

Table 2. FRET theory results for the compounds.

Type of Complex	R_0 (nm)	r (nm)	E
L	0.4682	0.4495	0.5608
MoL_2	0.5050	0.4004	0.8011

Table 3. DNA-binding constants, binding energy and the enhancement constant (K_E) of the compounds.

Type of Complex	$K_{binding}/M^{-1}$ (Fluorescence)	$K_{binding}/M^{-1}$ (UV-Vis)	Binding Energy/kcal.mol^{-1} (Docking)	$K_E/\mu M^{-1}$
L	9.6×10^3	1.7×10^3	-5.50	0.0705
MoL_2	1.5×10^5	1.9×10^3	-8.77	0.023

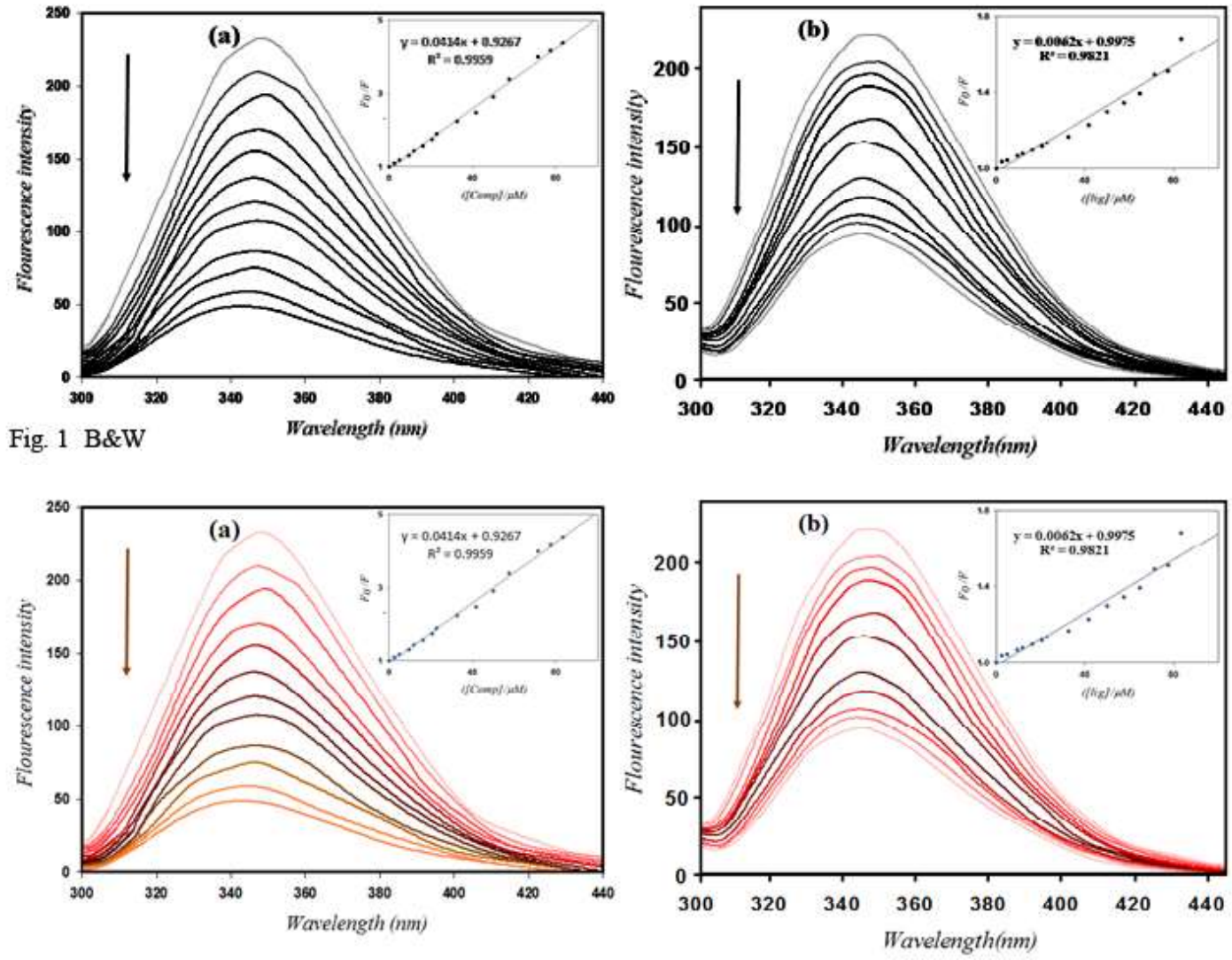

Fig. 1 B&W

Fig. 1. Chemical structure of (a) MOL_2, (b) L.

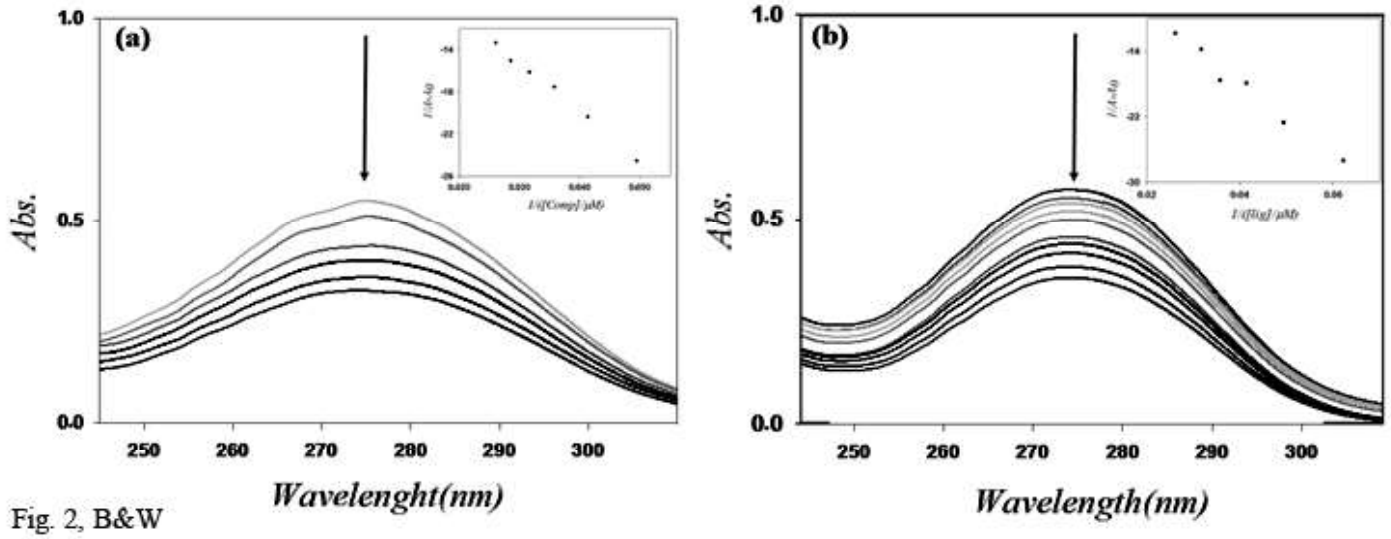

Fig. 2, B&W

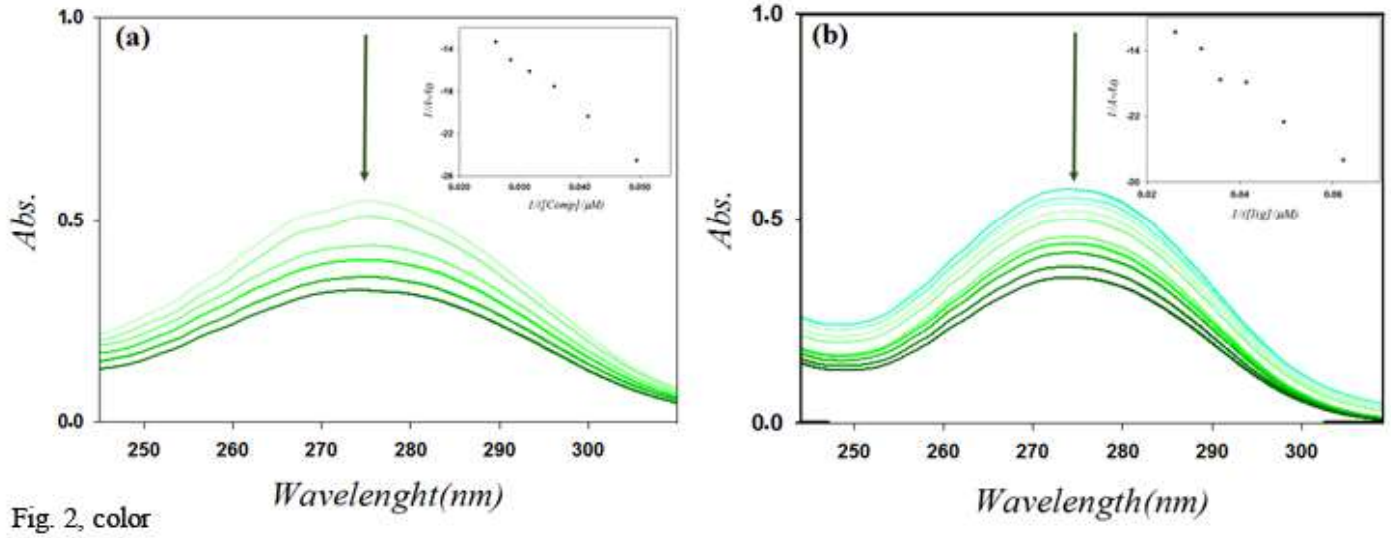

Fig. 2, color

Fig. 2. Fluorescence quenching of 5×10^{-6} M BSA in the presence of 0.5-50 μM of (a) **MoL_2**, (b) **L**.

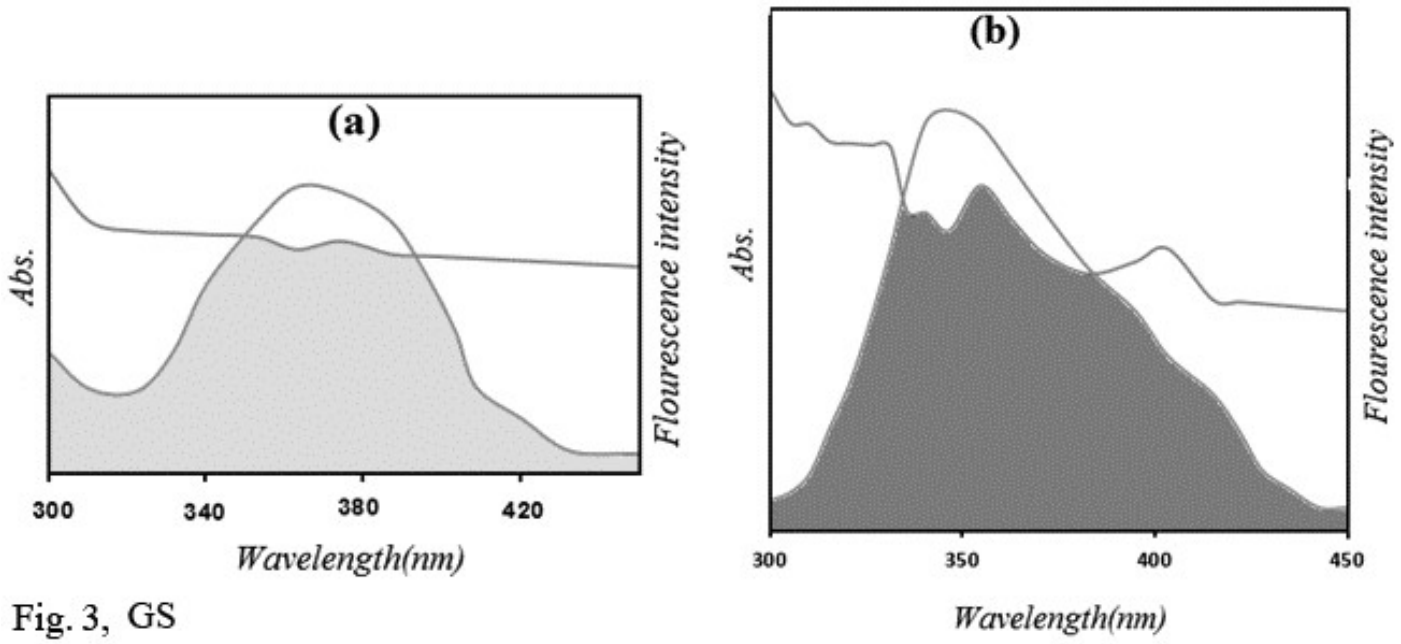

Fig. 3, GS

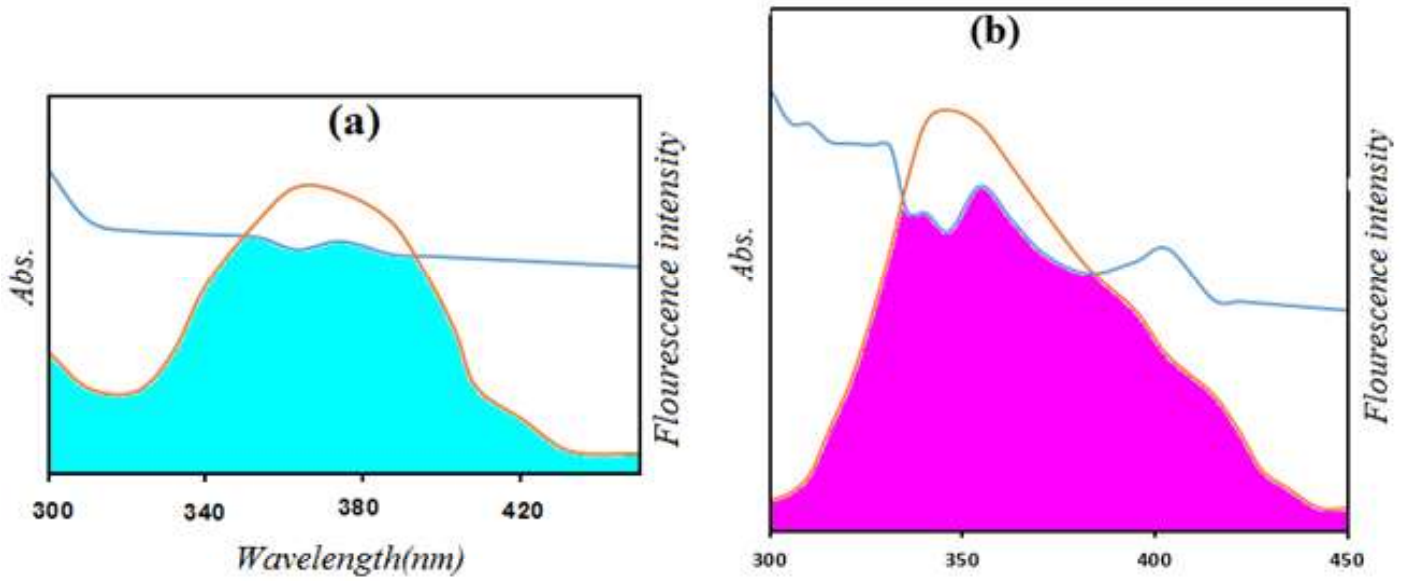

Fig. 3, color

Fig. 3. Electronic absorption spectra of BSA (10 mM) in the absence and presence of various concentrations of (a) **MoL_2** and (b) **L**.

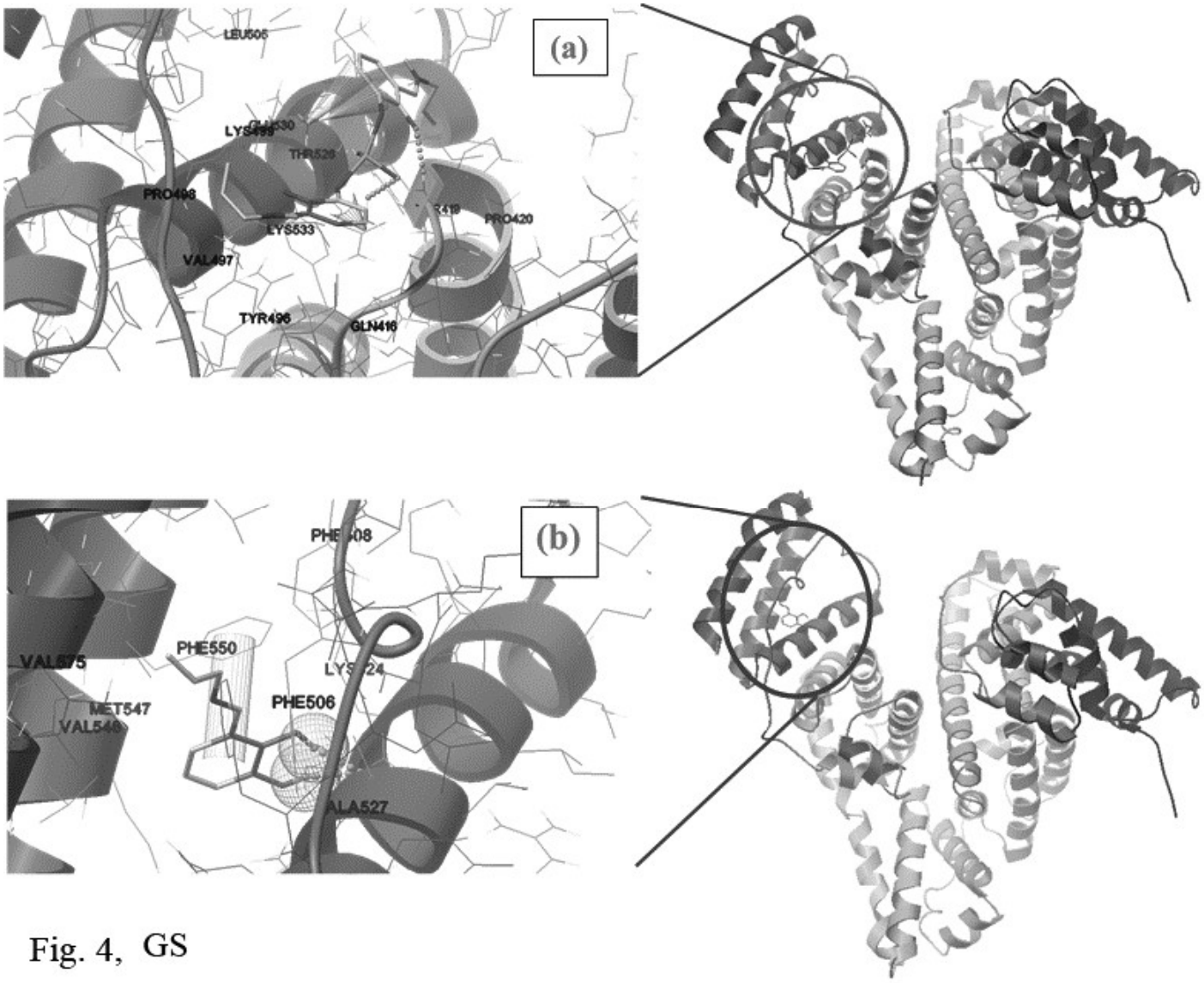

Fig. 4, GS

Fig. 4. Spectral overlap of the BSA fluorescence with the (a) $\mathbf{MoL_2}$ and (b) **L** absorption spectrum.

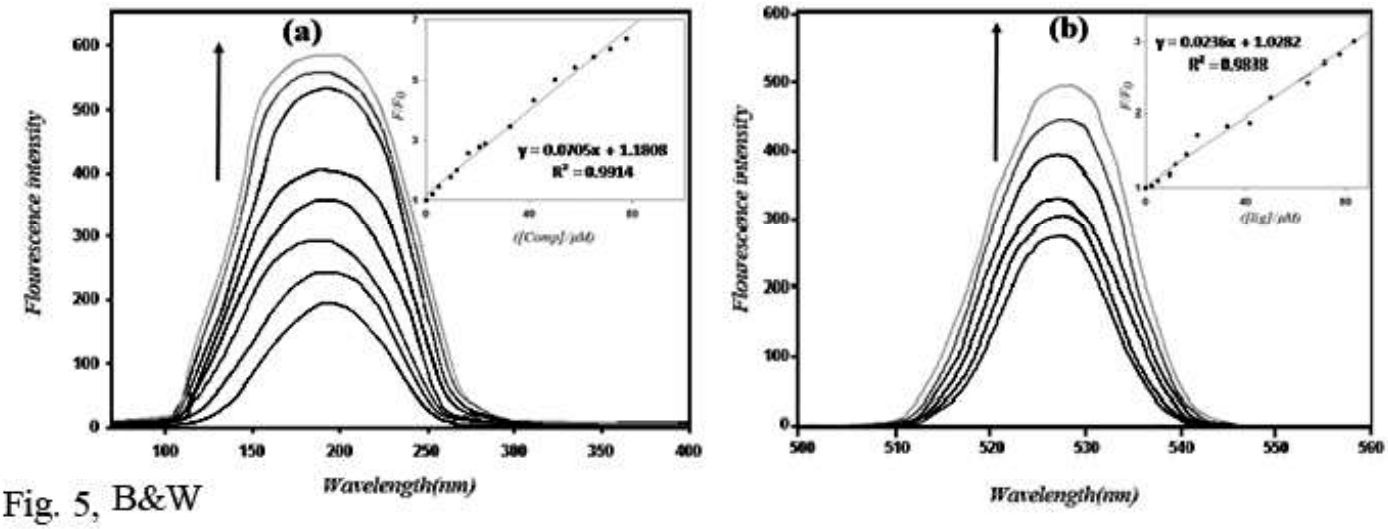

Fig. 5, B&W

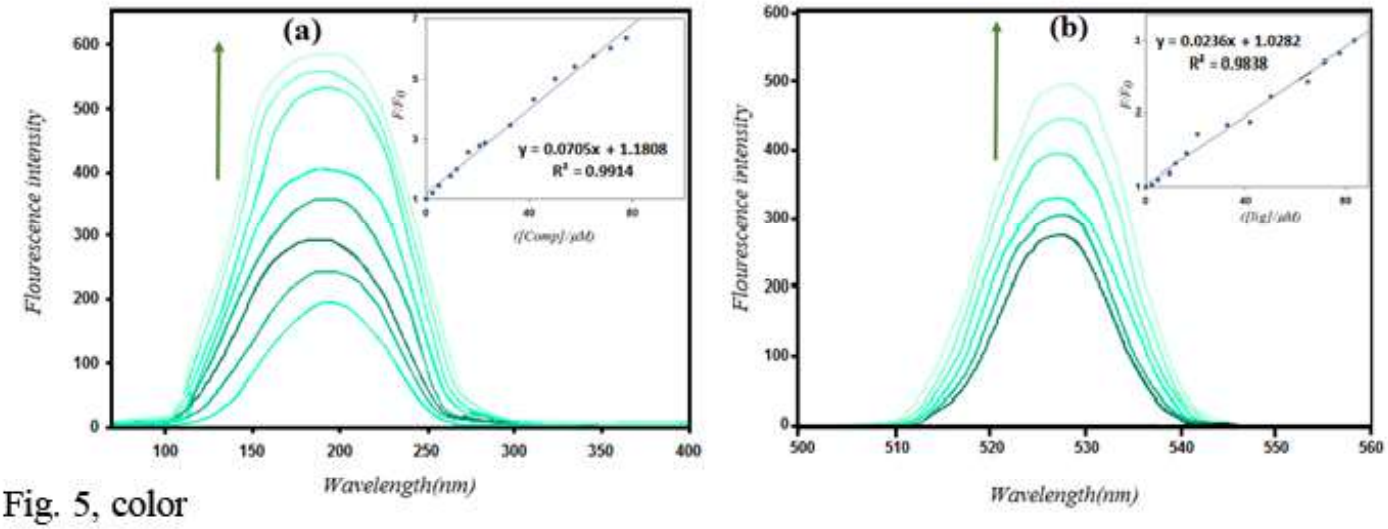

Fig. 5, color

Fig. 5. The docking diagrams of the BSA-compound complexes. a) **MoL_2** and b) **L**. Mo atom, Hydrogen bonds, π-cation and π-π interactions are shown as blue circle, green spheres, yellow cones and yellow cylinders, respectively.

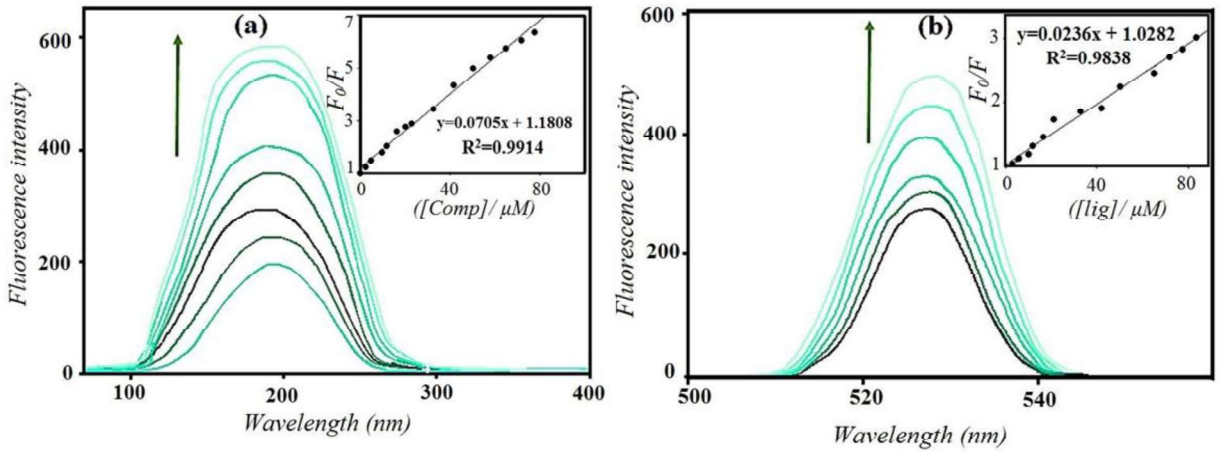

Fig. 6. Fluorescence enhancement of EtBr-DNA complex in the presence of various amounts of (a) $\mathbf{MoL_2}$, (b) **L**.

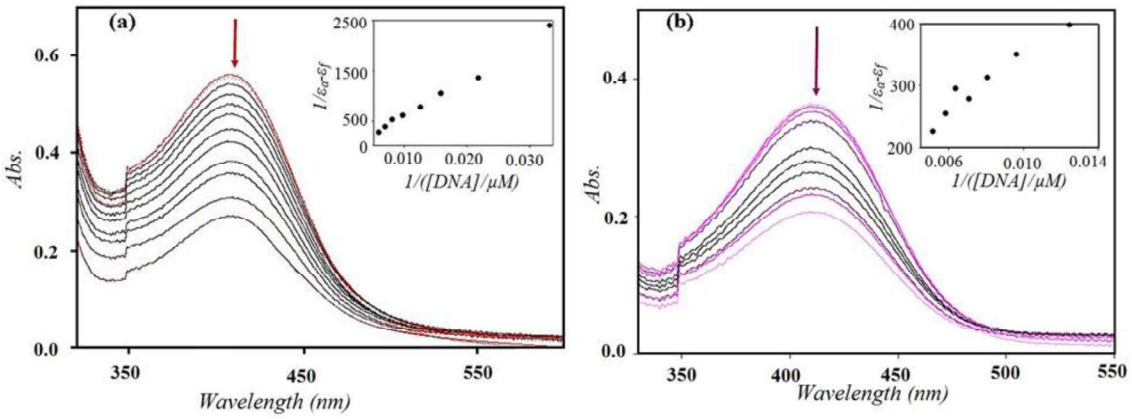

Fig. 7. Electronic absorption spectra of (a) $\mathbf{MoL_2}$ and (b) **L** in the absence and presence of various concentrations of DNA.

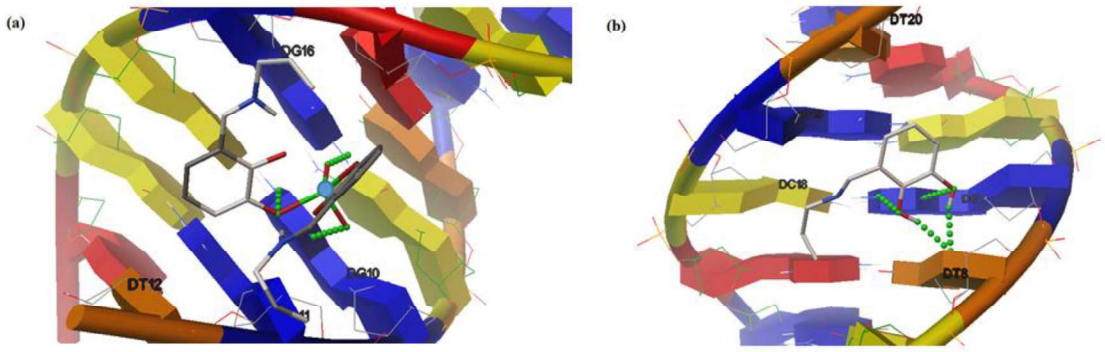

Fig. 8. The docking diagrams of the DNA-compound complexes. a) **MoL_2** and b) **L**. Mo atom and Hydrogen bond interactions are shown as blue circle and green spheres, respectively.